Optimal Control of Majorana Zero Modes

Torsten Karzig,[1] Armin Rahmani,[2,3] Felix von Oppen,[4] and Gil Refael[1]

[1]*Institute of Quantum Information and Matter, California Institute of Technology, Pasadena, California 91125, USA*
[2]*Theoretical Division, T-4 and CNLS, Los Alamos National Laboratory, Los Alamos, New Mexico 87545, USA*
[3]*Quantum Matter Institute, University of British Columbia, Vancouver, British Columbia, Canada V6T 1Z4*
[4]*Dahlem Center for Complex Quantum Systems and Fachbereich Physik, Freie Universität Berlin, 14195 Berlin, Germany*

(Dated: December 19, 2014)

Braiding of Majorana zero modes provides a promising platform for quantum information processing, which is topologically protected against errors. Strictly speaking, however, the scheme relies on infinite braiding times as it utilizes the adiabatic limit. Here we show how to minimize nonadiabatic errors for finite braiding times by finding an optimal protocol for the Majorana movement. Interestingly, these protocols are characterized by sharp transitions between Majorana motion at maximal and minimal velocities. We find that these so-called bang-bang protocols can minimize the nonadiabatic transitions of the system by orders of magnitude in comparison with naive protocols.

Topological quantum computing is a promising approach to quantum information processing, which provides remarkable robustness against errors [1, 2]. At the heart of this approach lie exotic quasiparticles known as non-Abelian anyons, which can emerge in several condensed matter systems; *adiabatic* exchange of such quasiparticles transforms the many-body wave function to a different degenerate wave function, in turn processing the information stored (nonlocally) in these quantum wave functions. In fact, adiabatic exchange, i.e., braiding, is the key ingredient of topological quantum computing. However, perfect adiabaticity requires infinite times. Therefore, it is imperative to be able to perform such transformations in finite time, while minimizing the undesirable nonadiabatic effects [3–7].

Majorana zero modes are one of the simplest and most important non-Abelian quasiparticle [8, 9]. There have been several proposals [10–14], as well as experimental progress [15–22], toward realizing these modes in one-dimensional hybrid systems, e.g., semiconducting quantum wires coupled to superconductors. Making a network of such quantum wires can in turn allow for braiding of these Majorana modes [23]. Thus, the minimal building block of quantum information processing with the quantum-wire incarnation of Majorana zero modes is moving them along the wire adiabatically. These zero modes are bound to domain walls between the topological and nontopological phases, whose position and velocity can be tuned externally, e.g., by means of gate electrodes. Adiabatic transport of the Majoranas then amounts to slowly moving these domain walls.

Consider a Majorana mode in a quantum wire bound to a domain wall at point A, with the system in one of its ground states (Fig. 1) and imagine moving the domain wall (and hence the associated Majorana mode) to point B a distance ℓ away within a prescribed time τ. What is the optimal choice for the time-dependent velocity of the domain wall? As this translation is carried out in finite time, there are deviations from the fully adiabatic evolution. We would like to choose a protocol which generates a state as close as possible to adiabatically moving the domain wall to point B. This is clearly important for realizations of topological quantum computers as both practical performance considerations and parasitic decoherence processes such as quasiparticle poisoning limit the available time for braiding processes [24–26].

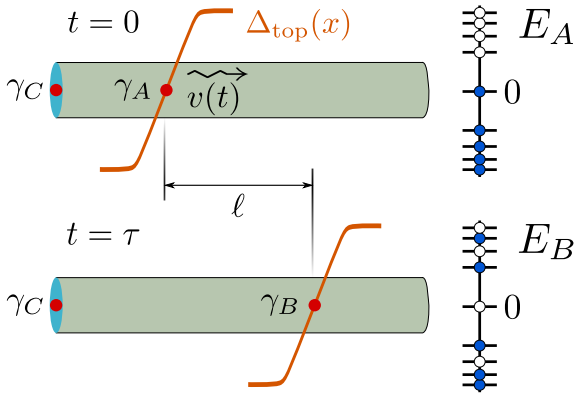

FIG. 1. Nonadiabatic motion of Majorana bound states. When moving a Majorana-carrying domain wall in a finite time τ by a distance ℓ, the final state will in general experience nonadiabatic excitations as indicated by the difference in the occupation of the low energy bound states, before (upper panel, $t = 0$, position A), and after (lower panel, $t = \tau$, position B) the motion.

More broadly, optimal control has emerged as a new direction in quantum dynamics [27–36]. By finding the *best* protocols to optimize a certain figure of merit, quantum optimal control paves the way towards harnessing the power of quantum evolution. While the primary motivation for the field comes from experimental advances with ultracold atoms, the applicability of quantum optimal control goes well beyond these systems. The subject of this paper, i.e., finding the optimal protocol to move a Majorana mode along a quantum wire, shows that optimal control can play an important role in topological quantum computing.

Figure of merit.—We start by defining an appropriate figure of merit. A very natural choice in the present case is to minimize

$$c(\tau) = 1 - |\langle \Psi_B^{\rm ad} | \Psi(\tau) \rangle|^2, \tag{1}$$

which quantifies the deviations from the adiabatic evolution

in terms of the squared overlap between $|\Psi(\tau)\rangle = U(\tau)|\Psi(0)\rangle$, the many-body wave function obtained after the quantum evolution for a time τ [with evolution operator $U(\tau)$], and $|\Psi_B^{\rm ad}\rangle$, the wave function after a perfectly adiabatic evolution. In the present case, $|\Psi_B^{\rm ad}\rangle$ is simply the ground state of the Hamiltonian with the domain wall at position B, while the initial state $|\Psi(0)\rangle$ is the ground state with the domain wall at point A.

Strictly speaking, the topological protection is lost once entering the nonadiabatic regime. If the system strays too far from the instantaneous ground state, the exponential protection originating from having well separated Majorana modes will be lost. One way to deal with this problem would be to use a figure of merit that rewards proximity to the ground state during the entire evolution. Here, we implement this by considering permissible velocities $v(t) < v_{\rm max}$ in such a way that we are never too far from the adiabatic limit. In this regime, most excitations occur within the bound-state spectrum of the domain wall which can be corrected without losing the topological protection.

We use Monte Carlo calculations (simulated annealing) to find the optimal protocol which minimizes the cost function in Eq. (1) for a fixed total time τ, average velocity ℓ/τ, and maximal velocity $v_{\rm max}$. This method finds the optimal protocol without making any *a priori* assumptions. Remarkably, we find that the optimal protocols have a bang-bang form, i.e., they are a sequence of sudden quenches between the maximal ($v_{\rm max}$) and the minimal (0) allowed velocities. Despite ubiquitously occurring in optimal control theory [28], such bang-bang protocols appear quite counterintuitive in the present context. Nevertheless, we find that they reduce the nonadiabatic errors by orders of magnitude in comparison with simple nonoptimal protocols, which one may construct intuitively (see Figure 2). In addition to our numerical results, which are obtained for specific models of the domain wall, we also adapt Pontryagin's maximum principle to our problem and establish more generally that the optimal protocols must be bang-bang.

Model.—We consider the effective Hamiltonian for a quantum wire (or topological insulator edge) [10–12] in the vicinity of a topological domain wall, assuming that the gap varies linearly as function of position [5]

$$\hat{H} = \int \hat{\Psi}^\dagger(x)\mathcal{H}\hat{\Psi}(x)dx, \quad \mathcal{H} = -iu\partial_x\sigma_z - b(x-y)\sigma_x. \quad (2)$$

Here, σ_i are Pauli matrices and $\hat{\Psi}^\dagger(x) = \left(\hat{\psi}_\uparrow^\dagger(x) + \hat{\psi}_\uparrow(x), \hat{\psi}_\downarrow^\dagger(x) - \hat{\psi}_\downarrow(x)\right)$ with $\hat{\psi}_\uparrow(x)$ $[\hat{\psi}_\downarrow(x)]$ representing the fermionic annihilation operator of spin up (down) electrons at position x. The parameter y denotes the position of the domain wall and is time dependent when the domain wall is moving along the wire.

For fixed y, the above Hamiltonian gives rise to single-particle bound states $\hat{\gamma}_{n,y}$ localized at $x = y$ with the spectrum $\varepsilon_n = \mathrm{sign}(n)\sqrt{|n|}\omega$, where n runs from $-\infty$ to ∞. The corresponding wave functions $\phi_n = (\mathrm{i} + \sigma_x)(\mathrm{sign}(n)g_{|n|-1}, g_{|n|})/2$ are given in terms of harmonic oscillator eigenstates $g_k(x-y)$ with frequency $\omega = \sqrt{2ub}$ and oscillator length $\xi = \sqrt{u/b}$. It can be shown that the zero-energy state ϕ_0 is a Majorana state

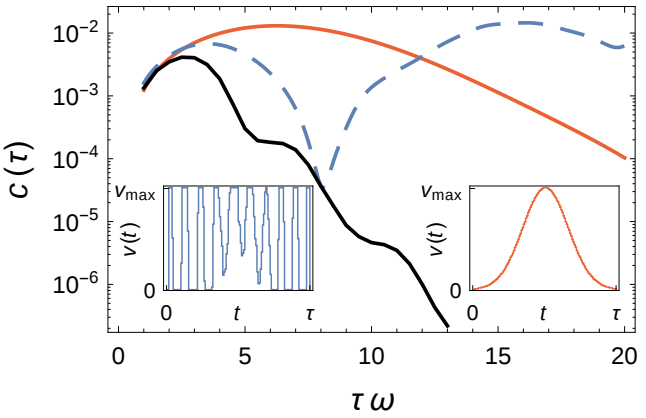

FIG. 2. Cost function for bang-bang-type optimal protocols (Gaussian reference protocol) shown in black (red) as a function of τ (with fixed average and maximum velocity). Optimal protocols were individually obtained for each τ (left inset shows a protocol optimized for $\tau = 8/\omega$), while the reference protocol is a smooth Gaussian curve shown in the right inset. The cost function $c(\tau)$ can be reduced by several orders of magnitude when using optimal protocols. The dashed blue curve shows the cost function obtained by applying the optimal protocol shape corresponding to $\tau = 8/\omega$ to other times. It outperforms the reference protocol for a wide time interval. Numerical parameters used: $v_{\rm max} = 0.3u$, $N = 128$, $n_{\rm max} = 30$, $n_c = 7$.

with quasiparticle operator $\hat{\gamma}_{0,y} = \hat{\gamma}_{0,y}^\dagger$ [5]. We assume that the domain wall is initially at $y(0) = 0$ (point A). The velocity $v(t) = \frac{d}{dt}y(t)$ of the domain wall is then subject to the following constraints: $0 \leqslant v(t) \leqslant v_{\rm max}$ and $y(\tau) = \int_0^\tau dt v(t) = \ell$. To avoid the strongly nonadiabatic regime, where the bound states become unstable [5], we work in the regime $v_{\rm max} \ll u$.

Evaluating the many-body overlap $|\langle\Psi_B^{\rm ad}|\Psi(\tau)\rangle|^2$ can be conveniently done in the Heisenberg picture by rewriting it as an expectation value of the Heisenberg evolved projector $|\Psi_B^{\rm ad}\rangle\langle\Psi_B^{\rm ad}| = \Pi_{i\leq 0}\hat{n}_i$. Here, $\hat{n}_{i\neq 0} = \hat{\gamma}_{i,B}^\dagger\hat{\gamma}_{i,B}$ is the occupation number of the finite-energy bound states and we defined the delocalized fermionic zero mode $\hat{d}_0 = (\hat{\gamma}_{0,B} + \mathrm{i}\hat{\gamma}_{0,C})/\sqrt{2}$. Then, we define the corresponding occupation number $\hat{n}_{0_-} = \hat{d}_0^\dagger\hat{d}_0$, assuming $\langle\Psi_B^{\rm ad}|\hat{n}_{0_-}|\Psi_B^{\rm ad}\rangle = 1$ without loss of generality. Here, we have added the minus subscript to indicate that $\hat{n}_{0_-}$ should be treated in analogy with the other negative-energy states. Along the same lines, we can define $\hat{n}_{0_+} = \hat{d}_0\hat{d}_0^\dagger$ which describes the occupation of the particle-hole conjugate "positive energy" state. Note that we focus here on the movement of a single domain wall where the far-away Majorana mode $\hat{\gamma}_{0,C}$ is static and does not contribute to nonadiabatic excitations.

For small maximal velocities $v_{\rm max}$, the occupation numbers $\hat{n}_{i\leq 0}$ are still close to unity, which allows for an expansion of $\hat{n}_{-i} = 1 - \hat{n}_i$ in small $\hat{n}_i$ (with $i \geq 0_+$). The cost function can then be approximated by

$$c(\tau) \approx \sum_{i\geq 0_+}\langle\hat{n}_i\rangle_\tau - \sum_{j>i,\, i\geq 0_+}\langle\hat{n}_i\hat{n}_j\rangle_\tau\,, \quad (3)$$

which may be evaluated straightforwardly with the knowledge of the Heisenberg evolution of the operators $\hat{\gamma}_{n,B}$ (and $\hat{d}_0$).

We evaluate the latter by approximating the protocol for moving the domain wall by a piece-wise constant sequence of velocities v_i (each of duration δt) for $i = 1 \dots N$. For each piece, the time evolution can be described by a mapping to the static case by a Lorentz boost, with boosted bound-state wavefunctions $\phi_n^{(v_i)}(x - v_i t)$ and a renormalized spectrum $\varepsilon_n^{(v_i)}$ [5] (see also Supplemental Information). With these exact constant-velocity solutions, the Heisenberg evolution of the domain wall bound states takes the form

$$U(\tau)^\dagger \hat{\gamma}_{n,B} U(\tau) = \sum_{\{m_i\}} a^{(v_N)}_{n,m_N} \dots a^{(v_1)}_{m_2,m_1} \hat{\gamma}_{m_1,A}, \qquad (4)$$

where $U(\tau)$ is the full many body time evolution operator and $a^{(v)}_{n,m} = \sum_k \langle \phi^{(0)}_n | \phi^{(v)}_k \rangle \langle \phi^{(v)}_k | \phi^{(0)}_m \rangle \exp(-\mathrm{i}\varepsilon^{(v)}_k \delta t)$. The matrix elements $\langle \phi^{(0)}_n | \phi^{(v)}_k \rangle$ are essentially overlaps of harmonic oscillator wavefunctions shifted by $\sim \sqrt{k} v/u\xi$ relative to each other. For small velocities, we have $\langle \phi^{(0)}_n | \phi^{(v)}_k \rangle \propto (v/u)^{(|n|-|k|)}$ [37]. The sums over the states (denoted by the indices k and m_i) can thus be cut off at $n_{\max} \gg n$ for numerical evaluations.

In fact, the same small-velocity limit also implies that the expansion in Eq. (3) is ultimately controlled by v/u, which enters with higher powers the more nontrivial transitions of the form (4) (with $m_1 \neq n$) are needed to transform products of occupation number operators of unoccupied states $\Pi_{i \geq 0_+} \hat{n}_i$ to that of occupied states during the Heisenberg evolution. Note that both terms in Eq. (3) only require two such transitions and are therefore of the same order, and more relevant than other terms involving three and more occupation number operators. (For more details see Supplemental Information.)

Optimization.—Based on the cost function (3), we use simulated annealing to find the optimal protocol [30, 38]. In this method, we fix the total time τ and distance ℓ and use a piecewise-constant protocol with N pieces of duration $\delta t = \tau/N$. (We then increase N systematically until convergence). We implement the constraint of a fixed average velocity in each Monte Carlo step by increasing the velocity of one randomly chosen interval while decreasing the velocity of another by the same amount. If the change Δc in the cost function is negative, we accept the move. Otherwise, we accept it with probability $e^{-\Delta c/T_{MC}}$, where T_{MC} is a fictitious temperature that is gradually reduced to zero.

As mentioned above, we only include $n_{\max}$ bound states in the numerical optimization. This makes the time evolution of states close to $n_{\max}$ unreliable. Observables such as the cost function should therefore be evaluated using a smaller cutoff $n_c \ll n_{\max}$ (restricting the sums in Eq. (3) to $i \leq n_c$). The results are independent of $n_{\max}$ as long as it is adequately large for a given n_c. On the other hand, n_c has physical significance. We are minimizing the excitations within the bound-state spectrum, while neglecting the saturation of domain $\Delta_{\mathrm{top}}(x) = bx$ away from the domain wall (see Fig. 1). A realistic domain wall binds a finite number of bound states n_{b}. It is then natural to choose $n_c = n_{\mathrm{b}}$ so that the optimization is aimed at conserving the overall parity of the bound states, which ultimately protects the Majorana qubit [39]. The states

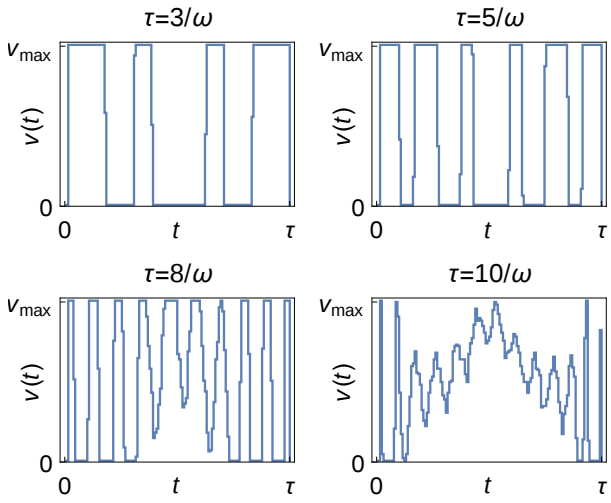

FIG. 3. Optimal bang-bang-type protocols for different durations τ. The number of bangs increases with τ. Due to the finite number of time steps, here $N = 128$, this leads to numerical artifacts for large times where size of the bangs reaches the time step width δt. The optimal protocols are then smoothed out because of an effective averaging over times δt. Further numerical parameters used: $v_{\max} = 0.3u$, $n_{\max} = 30$, $n_c = 7$.

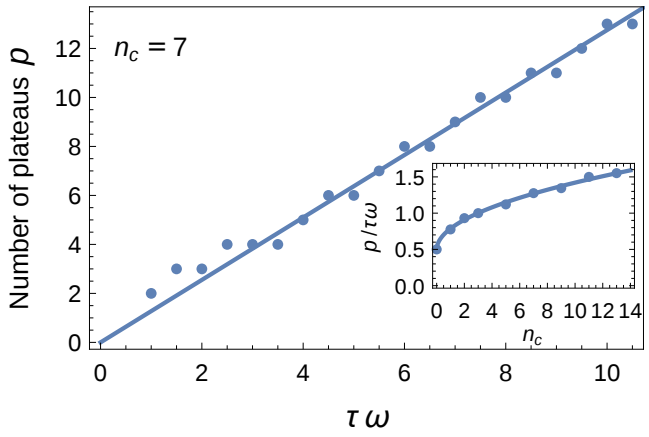

FIG. 4. Dependence of the bang-bang-type protocols on the duration τ. The number of plateaus with high velocity p scales linearly to the protocol duration τ. The inset shows the change of the slope $p/\tau\omega$ with the number of bound states in the cost function n_c. A fit to our data shows that it can be well approximated by $p/\tau\omega = 0.3\sqrt{n_c}+0.5$.

$|n| > n_c$ that are left out from the optimization would represent high-energy continuum states. Possible (although unlikely) nonadiabatic transitions within these states, e.g., creation of a high energy particle-hole pair, do not change the parity of the bound states. We assume that these excitations are dissipated on a length scale which is shorter than the distance between Majorana modes, which allows us to use our local optimization procedure.

Results.—The central result of our Monte Carlo simulations is that the optimal protocols are of bang-bang character and outperform naive protocols by orders of magnitude

(see Fig. 2). The sharp bang-bang transitions can be very well resolved numerically for not-too-large τ (see Fig. 3). For a fixed number of velocity steps N, the time resolution decreases for larger τ. Once the minimal time steps $\delta t = \tau/N$ exceed the interval between consecutive velocity jumps of the optimal protocols, the numerics average the optimal protocol over times δt resulting in a smoothing of the bang-bang character. Thus, when taking the adiabatic limit $\tau \to \infty$ before increasing $N \to \infty$, the optimal protocols become smooth and are determined by the density of underlying high-velocity sections.

For good time resolutions, the main characteristic of the optimal protocols is the number p of high-velocity plateaus. Interestingly, p is independent of many of the specifics of the braiding process such as the maximal velocity $v_{\max}$ and the displacement ℓ (controlling the average velocity for fixed τ), which only change the size of the plateaus. Instead, we find that p is determined by the domain-wall spectrum. More specifically, p/τ is of the order of the bound state energy (see Fig. 4). In a simple picture, the bang-bang protocols can be thought of as well timed echos that reverse the nonadiabatic evolution. From this point of view, it is natural to assume that the relevant scale for this timing is given by the energy of the excited bound states. This is in line with the approximate $p/\tau \sim \omega\sqrt{n_c} = \varepsilon_{n_c}$ behavior that we observe in our simulations (see Fig. 4). We will see below that $\omega\sqrt{n_c}$ also appears as a characteristic frequency scale of the corresponding Pontryagin equations that describe the optimal protocol.

Although the form of the protocols does not converge for large n_c, the changes become less and less important for the cost function. Our data indicate (see Supplemental Information) that $c(\tau)$ saturates for large n_c. Similarly, when applying the cost function (with fixed n_c) to protocols optimized for "wrong" values of n_c', their performance is still very close to the $n_c' = n_c$ case for not too small values of n_c', n_c. Specifically, even though a large n_c yields an optimal protocol with large p, it can still be well approximated by a protocol with fewer bangs that would be obtained when choosing a smaller n_c'. All these observations reflect the weak occupation of states with large quantum numbers due to the close-to-adiabatic regime.

Pontryagin equation.—The bang-bang nature of the protocols can be understood in terms of Potryagin's principle [40], which is a generalization of the Euler-Lagrange equations. We briefly review the formalism. Assume we want to find the optimal control $v^*(t)$ that minimizes a cost function $c(\{x(\tau)\}) + \int_0^\tau \mathcal{L}(\{x\}, v)dt$ for a set of dynamical variables $\{x(t)\}$ evolving with the equations of motion $\dot{x}_j = f_j(\{x\}, v)$, boundary conditions $x_j(0) = x_j^0$, and permissible control $v(t)$. The function $c(\{x(\tau)\})$ only depends on the final values of the dynamical variables at $t = \tau$, while the additional integral over $\mathcal{L}(\{x\}, v)$ allows for dependence on the entire trajectory. We can think of the equations of motion above as constraints that can be implemented by Lagrange multipliers $p_j(t)$ (hereafter referred to as conjugate momenta) at every point in time by adding $\sum_j \int_0^\tau dt p_j \left[f_j(\{x\}, v) - \dot{x}_j\right]$ to the cost function. Calculus of variations then implies the following equations of motion for the conjugate momenta: $\dot{p}_j = -\frac{\partial \mathscr{H}}{\partial x_j}$, with boundary condition $p_j(\tau) = \frac{\partial}{\partial x_j} c(\{x(\tau)\})$, where the *optimal-control Hamiltonian* is constructed as

$$\mathscr{H}(\{x, p\}, v) = \mathcal{L}(\{x\}, v) + \sum_j p_j f_j(\{x\}, v). \tag{5}$$

The optimal control $v^*(t)$ and the corresponding $\{x^*, p^*\}$ then satisfy $\mathscr{H}(\{x^*, p^*\}, v^*) = \min_{\{v\}} \mathscr{H}(\{x^*, p^*\}, v)$.

In the present case, we have a very similar problem: The control parameter is the velocity $v(t)$ of the domain wall for $0 < t < \tau$ and the dynamical variables constitute a parameterization of the time-dependent wave function of the system. For example, we can expand the single-particle wave function corresponding to level m as

$$\psi^m(x, t) = \sum_n \left(\varphi_n^m(t),\ \theta_n^m(t)\right) g_n(x - y). \tag{6}$$

The shift of $y(t)$ to the instantaneous position of the domain wall allows us to readily relate the dynamical variables, i.e., the real and imaginary parts of φ_n^m and θ_n^m, to $|\Psi_B^{\mathrm{ad}}\rangle$. Therefore, the cost function $c(\tau)$ [see Eq. (1)] can be easily obtained from the final values of these dynamical variables.

Our physical cost function $c(\tau)$ only depends on the final values of the dynamical variables (no dependence on trajectory). However, compared with the standard formalism, we have one additional constraint, namely, a fixed total displacement ℓ, which can be accounted for by adding a Lagrange-multiplier term $\lambda\left(\int_0^\tau v(t)dt - \ell\right)$ to the cost function. Interestingly, this constraint adds a linear term in v to the optimal-control Hamiltonian, i.e., $\mathcal{L}(\{x\}, v) = \lambda v$ [see Eq. (5)]. The equations of motion for the dynamical variables are also linear in v:

$$\begin{aligned}\dot{\varphi}_n^m = \frac{\omega}{2}(v/u - 1)\left(\sqrt{n+1}\varphi_{n+1}^m - \sqrt{n}\varphi_{n-1}^m\right) \\ + i\frac{\omega}{2}\left(\sqrt{n+1}\theta_{n+1}^m + \sqrt{n}\theta_{n-1}^m\right),\end{aligned} \tag{7}$$

and a similar expression with $v/u - 1 \to v/u + 1$ and $\varphi \leftrightarrow \theta$ for $\dot{\theta}_n^m$ (notice that the dependence on m is only through the initial conditions).

Therefore, the optimal-control Hamiltonian $\mathscr{H}$ is linear in v and the condition given below Eq. (5) for v^* can only be satisfied if $v(t)$ takes its minimum or maximum permissible value as determined by the sign of the coefficient of v [i.e., $\mathrm{sgn}(\partial_v \mathscr{H})$] unless $\partial_v \mathscr{H} = 0$ over finite intervals. We have checked explicitly that the discontinuities in our protocols do indeed coincide with zeros of $\partial_v \mathscr{H}$ (see the Supplemental Material). Also notice that the distance between these zeros (typical duration of a bang) is determined by the oscillations of $\mathscr{H}$, which originate from the oscillations of the dynamical variables and their conjugate momenta. The appearance of $\omega\sqrt{n}$ in the equations of motion (7) provides further support for the observed behavior $p/\tau \sim \omega\sqrt{n_c}$ (see Fig. 4).

Conclusions.—As a first application of optimal control to braiding non-Abelian anyons, we obtained bang-bang protocols that can move Majorana zero modes along a quantum

wire in *finite* times, while reducing the associated nonadiabatic errors by orders of magnitude (compared with naive smooth protocols). Our calculations were based on a figure of merit that maximizes the magnitude of the overlap between the resulting wave function and the adiabatic one. While more sophisticated cost functions might be needed to account for, e.g., phase errors in a realistic braiding process, our results suggest that optimal control could play an important role in topological quantum computing. Adiabatic braiding can achieve remarkable robustness at the expense of performance. By beating the barrier of adiabaticity, our optimal-control approach may foster the development of high-performance topological quantum computers.

We acknowledge valuable discussions with Chang-Yu Hou and Falko Pientka. This work was funded by the Packard Foundation and the Institute for Quantum Information and Matter, an NSF Physics Frontiers Center with support of the Gordon and Betty Moore Foundation through Grant GBMF1250 (TK,GR). We also acknowledge support from the U.S. DOE through LANL/LDRD program, NSERC, CIfAR and Max Planck - UBC Centre for Quantum Materials (AR) as well as the Helmholtz Virtual Institute "New states of matter and their excitations" and SPP1285 of the Deutsche Forschungsgemeinschaft (FvO).

[1] A. Kitaev, Ann. Phys. **303**, 2 (2003).
[2] C. Nayak, S. H. Simon, A. Stern, M. Freedman, and S. Das Sarma, Rev. Mod. Phys. **80**, 1083 (2008).
[3] M. Cheng, V. Galitski, and S. Das Sarma, Phys. Rev. B **84**, 104529 (2011).
[4] E. Perfetto, Phys. Rev. Lett. **110**, 087001 (2013).
[5] T. Karzig, G. Refael, and F. von Oppen, Phys. Rev. X **3**, 041017 (2013).
[6] M. S. Scheurer and A. Shnirman, Phys. Rev. B **88**, 064515 (2013).
[7] C. S. Amorim, K. Ebihara, A. Yamakage, Y. Tanaka, and M. Sato, arXiv:1405.5153 (2014).
[8] J. Alicea, Rep. Prog. Phys. **75**, 076501 (2012).
[9] C. Beenakker, Annu. Rev. Condens. Matter Phys. **4**, 113 (2013).
[10] L. Fu and C. L. Kane, Phys. Rev. Lett. **100**, 096407 (2008).
[11] R. M. Lutchyn, J. D. Sau, and S. Das Sarma, Phys. Rev. Lett. **105**, 077001 (2010).
[12] Y. Oreg, G. Refael, and F. von Oppen, Phys. Rev. Lett. **105**, 177002 (2010).
[13] M. Duckheim and P. W. Brouwer, Phys. Rev. B **83**, 054513 (2011).
[14] S. Nadj-Perge, I. K. Drozdov, B. A. Bernevig, and A. Yazdani, Phys. Rev. B **88**, 020407 (2013).
[15] V. Mourik, K. Zuo, S. M. Frolov, S. R. Plissard, E. P. a. M. Bakkers, and L. P. Kouwenhoven, Science **336**, 1003 (2012).
[16] A. Das, Y. Ronen, Y. Most, Y. Oreg, M. Heiblum, and H. Shtrikman, Nat. Phys. **8**, 887 (2012).
[17] M. T. Deng, C. L. Yu, G. Y. Huang, M. Larsson, P. Caroff, and H. Q. Xu, Nano Lett. **12**, 6414 (2012).
[18] L. P. Rokhinson, X. Liu, and J. K. Furdyna, Nat Phys **8**, 795 (2012).
[19] A. D. K. Finck, D. J. Van Harlingen, P. K. Mohseni, K. Jung, and X. Li, Phys. Rev. Lett. **110**, 126406 (2013).
[20] V. S. Pribiag, A. J. A. Beukman, F. Qu, M. C. Cassidy, C. Charpentier, W. Wegscheider, and L. P. Kouwenhoven, arXiv:1408.1701 (2014).
[21] S. Hart, H. Ren, T. Wagner, P. Leubner, M. Mühlbauer, C. Brüne, H. Buhmann, L. W. Molenkamp, and A. Yacoby, Nat Phys **10**, 638 (2014).
[22] S. Nadj-Perge, I. K. Drozdov, J. Li, H. Chen, S. Jeon, J. Seo, A. H. MacDonald, B. A. Bernevig, and A. Yazdani, Science **346**, 602 (2014).
[23] J. Alicea, Y. Oreg, G. Refael, F. von Oppen, and M. P. A. Fisher, Nat. Phys. **7**, 412 (2011).
[24] G. Goldstein and C. Chamon, Phys. Rev. B **84**, 205109 (2011).
[25] J. C. Budich, S. Walter, and B. Trauzettel, Phys. Rev. B **85**, 121405 (2012).
[26] D. Rainis and D. Loss, Phys. Rev. B **85**, 174533 (2012).
[27] U. Hohenester, P. K. Rekdal, A. Borzì, and J. Schmiedmayer, Phys. Rev. A **75**, 023602 (2007).
[28] P. Salamon, K. H. Hoffmann, Y. Rezek, and R. Kosloff, Phys. Chem. Chem. Phys. **11**, 1027 (2009).
[29] X. Chen, A. Ruschhaupt, S. Schmidt, A. del Campo, D. Guéry-Odelin, and J. G. Muga, Phys. Rev. Lett. **104**, 063002 (2010).
[30] A. Rahmani and C. Chamon, Phys. Rev. Lett. **107**, 016402 (2011).
[31] P. Doria, T. Calarco, and S. Montangero, Phys. Rev. Lett. **106**, 190501 (2011).
[32] T. Caneva, T. Calarco, R. Fazio, G. E. Santoro, and S. Montangero, Phys. Rev. A **84**, 012312 (2011).
[33] S. Choi, R. Onofrio, and B. Sundaram, Phys. Rev. A **84**, 051601 (2011).
[34] A. del Campo, EPL (Europhysics Letters) **96**, 60005 (2011).
[35] K. H. Hoffmann, P. Salamon, Y. Rezek, and R. Kosloff, EPL **96**, 60015 (2011).
[36] A. Rahmani, T. Kitagawa, E. Demler, and C. Chamon, Phys. Rev. A **87**, 043607 (2013).
[37] With the exception $\langle \phi_n^{(0)} | \phi_{-n}^{(v)} \rangle \propto (v/u)^2$. See also Supplemental Information.
[38] A. Rahmani, Mod. Phys. Lett. B **27**, 1330019 (2013).
[39] A. R. Akhmerov, Phys. Rev. B **82**, 020509 (2010).
[40] L. S. Pontryagin, *Mathematical Theory of Optimal Processes* (CRC Press, 1987).

Supplemental Information

S1: FINITE VELOCITY WAVEFUNCTIONS

The finite velocity bound state wavefunctions $\phi_n^{(v_i)}[x - y(t)]$ can be obtained by applying a Lorentz boost to Eq. (2) and take the form [5]

$$\phi_n^{(v)}(x) = \gamma^{1/4} \begin{pmatrix} \sqrt{1+v/u} & 0 \\ 0 & \sqrt{1-v/u} \end{pmatrix} \phi_n(\sqrt{\gamma}x)\, \mathrm{e}^{\mathrm{i}\sqrt{2\gamma n}(v/u)(x/\xi)}\,, \tag{S1}$$

where $\gamma = 1/\sqrt{1-(v/u)^2}$ and the renormalized bound state spectrum is given by $\varepsilon_n^{(v)} = \mathrm{sign}(n)\gamma^{-3/2}\sqrt{|n|}\omega$. The crucial difference of the finite-velocity, relative to the static bound states is the momentum boost of the form $\exp(\mathrm{i}qx)$. Since the ϕ_n consist of harmonic oscillator wavefunctions g_n the corresponding matrix elements $\langle\phi_k^{(v)}|\phi_n\rangle$ are controlled by integrals

$$\int \mathrm{d}x g_n(x) g_{n'}(x) \mathrm{e}^{-\mathrm{i}\sqrt{2}qx/\xi} = \mathrm{e}^{-\frac{1}{2}q^2}\sqrt{m!/M!}\,(-\mathrm{i}q)^{M-m} L_m^{M-m}\left(q^2\right), \tag{S2}$$

where $M = \max(n,n')$, $m = \min(n,n')$, and L_m^{M-m} are associated Laguerre polynomials. Since $L_m^{M-m}(q=0)$ just contributes with a constant one obtains by applying Eq. (S2) that

$$\langle\phi_k^{(v)}|\phi_n\rangle \propto (v/u)^{||k|-|n||} \tag{S3}$$

to leading order in v/u, with the exception of the $k = -n$ term that is proportional to $(v/u)^2$. Specifically, to linear order in v/u, we only obtain nonvanishing contributions

$$\langle\phi_k^{(v)}|\phi_n\rangle = \frac{1}{4}(-\mathrm{i}Mv/u)\left(1 + \mathrm{sign}(kn)\sqrt{(|M|-1)/|M|}\right) \quad, \text{if } ||k|-|n|| = 1\,, \tag{S4}$$

and $\langle\phi_k^{(v)}|\phi_n\rangle = 1 + \mathrm{sign}(kn)$, if $|k| = |n|$. Here, M is again given by the larger (in absolute value) of k and n.

S2: EVALUATION OF THE COST FUNCTION

To evaluate the cost function $c(\tau)$ it is helpful to express Eq. (3) explicitly in terms of the Heisenberg operators $\hat{\gamma}_i(\tau) = U(\tau)^\dagger \hat{\gamma}_{n,B} U(\tau)$,

$$c(T) = \sum_{i\geq 0_+} \left\langle \hat{\gamma}_{i,B}^\dagger(\tau)\hat{\gamma}_{i,B}(\tau)\right\rangle_0 - \sum_{j>i;\, i\geq 0_+} \left\langle \hat{\gamma}_{j,B}^\dagger(\tau)\hat{\gamma}_{i,B}^\dagger(\tau)\hat{\gamma}_{i,B}(\tau)\hat{\gamma}_{j,B}(\tau)\right\rangle_0 + \dots\,, \tag{S5}$$

where all expectation values $\langle\dots\rangle_0$ are taken with respect to the initial ground state with all states at $i \geq 0_+$ unoccupied. Note that we use the shorthand notation $\hat{\gamma}_{0_+,B} \equiv \hat{d}_0 = (\hat{\gamma}_{0,B} + \mathrm{i}\hat{\gamma}_{0,C})/\sqrt{2}$ and $\hat{\gamma}_{0_-,B} \equiv \hat{d}_0^\dagger$. From the normal ordered form of Eq. (S5) it becomes clear that nonvanishing contributions to the cost function $c(\tau)$ require transitions of initial $\hat{\gamma}_{i\geq 0_+,B}$ to final $\hat{\gamma}_{j\geq 0_+,A}^\dagger$ during the Heisenberg evolution (as mentioned in the main text). With the knowledge of the time evolution [see Eq. (4)] we can write $\hat{\gamma}_{i,B}(\tau) = \sum_j \alpha_{ij}\hat{\gamma}_{j,A}$, where the sum over j runs from $-n_{\max}$, over 0, to $+n_{\max}$. Note that there is a subtlety in treating the zero modes. To transform from the basis using the Majorana operators $\hat{\gamma}_{0,B}$ to the fermionic zero modes $\hat{\gamma}_{0_\pm,B}$ used in Eq. (S5) we define the $(2n_{\max}+2)\times(2n_{\max}+2)$ dimensional matrix $\tilde{\alpha}_{nm}$ such that

$$\begin{pmatrix} \hat{\gamma}_{n>0,B}(\tau) \\ \hat{d}_0(\tau) \\ \hat{d}_0^\dagger(\tau) \\ \hat{\gamma}_{n<0,B}(\tau) \end{pmatrix} = \sum_m \underbrace{\begin{pmatrix} \alpha_{nm} & \frac{1}{\sqrt{2}}\alpha_{n,0} & \frac{1}{\sqrt{2}}\alpha_{n,0} & \alpha_{nm} \\ \frac{1}{\sqrt{2}}\alpha_{0,m} & \frac{\alpha_{00}+1}{2} & \frac{\alpha_{00}-1}{2} & \frac{1}{\sqrt{2}}\alpha_{0,m} \\ \frac{1}{\sqrt{2}}\alpha_{0,m} & \frac{\alpha_{00}-1}{2} & \frac{\alpha_{00}+1}{2} & \frac{1}{\sqrt{2}}\alpha_{0,m} \\ \alpha_{nm} & \frac{1}{\sqrt{2}}\alpha_{n,0} & \frac{1}{\sqrt{2}}\alpha_{n,0} & \alpha_{nm} \end{pmatrix}}_{\tilde{\alpha}_{nm}} \begin{pmatrix} \hat{\gamma}_{m>0,A} \\ \hat{d}_0 \\ \hat{d}_0^\dagger \\ \hat{\gamma}_{m<0,A} \end{pmatrix}. \tag{S6}$$

This allows to express the cost function as

$$c(\tau) = \sum_{i,j\geq 0_+} \tilde{\alpha}_{-i,j}\tilde{\alpha}_{i,-j} - \sum_{i>j;\, i,j,k,l\geq 0_+} \left(\tilde{\alpha}_{-j,k}\tilde{\alpha}_{-i,-k}\tilde{\alpha}_{i,l}\tilde{\alpha}_{j,-l} + \tilde{\alpha}_{-j,k}\tilde{\alpha}_{-i,l}\tilde{\alpha}_{i,-l}\tilde{\alpha}_{j,-k} - \tilde{\alpha}_{-j,k}\tilde{\alpha}_{-i,l}\tilde{\alpha}_{i,-k}\tilde{\alpha}_{j,-l}\right) + \dots \tag{S7}$$

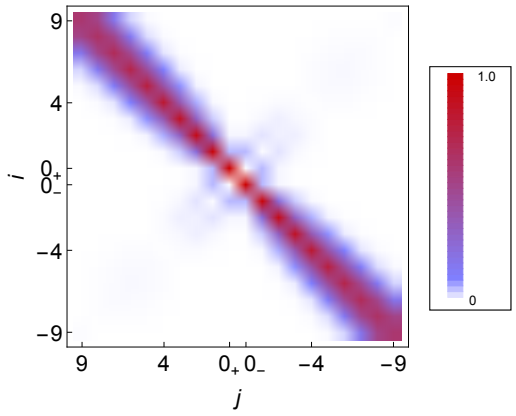

FIG. S1. Array plot of the matrix $|\tilde{\alpha}_{ij}|$ describing the Heisenberg time evolution as $\hat{\gamma}_{i,B}(\tau) = \sum_j \tilde{\alpha}_{ij}\hat{\gamma}_{j,A}$. The corresponding protocol is an optimal bang-bang protocol depicted in Fig. 3 with $\tau = 3/\omega$, $v_{\max} = 0.3u$, $n_{\max} = 30$, and $n_c = 7$.

As mentioned in the main text the expansion of Eq. (S7) is ultimately controlled by the velocity of the domain wall v. For small v/u the matrix $\tilde{\alpha}_{ij}$ is mainly diagonal as the off-diagonal terms are suppressed by powers of (v/u) [see Eq. (S3)]. One can therefore obtain an estimate of the importance of the different terms in Eq. (S7) by counting orders of v/u. The first term involves two off-diagonal elements and is therefore of order $(v/u)^2$. Interestingly, the second term is of the same order since for $k = i = l$ it takes the same form and is only smaller by a factor of two than the first term because of the restriction of the sum to $i > j$. The third and fourth terms are already of order $(v/u)^4$. By writing higher order terms, e.g., $\langle \delta n_i \delta n_j \delta n_k \rangle$ in normal ordered form similar to Eq. (S5), one can quickly show that they are also suppressed by at least $(v/u)^4$ which justifies Eq. (3).

Note that although the small v/u limit gives a convenient way to quantify the above expansion, the approximation remains well justified even for moderate v/u as long as the time evolution does not create too many excitations. In fact moderate v/u allow values of $\tilde{\alpha}_{i,j}$ to be of order 1 even for $i \neq j$ as long as i and j both have the same sign. However, due to the Pauli principle, these processes cannot cause changes in the occupation numbers which require transitions from negative to positive energy states. The latter are still rare for not too non-adiabatic evolutions as can be seen from the suppression of the off-diagonal blocks in Fig. S1 (see also Eq. (S4). On can then use the number of occurrences of $\tilde{\alpha}_{i,j}$ with $\mathrm{sign}(ij) = -1$ in Eq. (S7) to replace the small parameter v/u, which yields the same terms in the expansion.

S3: EFFECT OF THE BOUND STATE NUMBER n_c

As mentioned in the main text the number of high velocity plateaus p increases when taking into account an increasing number of bound states n_c in the optimization scheme. The lack of protocol convergence for $n_c \to \infty$ might seem surprising at first but is not problematic because of the decreasing importance of the protocol change. The left panel of Fig. S2 suggests that the cost function saturates in the $n_c \to \infty$ limit. Moreover, when measuring the protocol performance with respect to a number of bound states n_c, it might even be sufficient to optimize the protocols for a different n_c' and still obtain similarly good results. This is shown in the right panel of Fig. S2. Both of these observations reflect the fact that the leading error that contributes to the cost function is caused by excitations of low energy states (roughly $n_c \lesssim 5$ in this case). Once the optimization addresses these leading contributions the cost function starts saturating.

S4: CONNECTION WITH PONTRYAGIN'S MAXIMUM PRINCIPLE

As discussed in the main text, the bang-bang nature of the protocols can be understood in terms of Pontryagin's theorem. Since we have a large number of dynamical variables $\mathrm{Re}(\varphi_n^m)$, $\mathrm{Re}(\theta_n^m)$, $\mathrm{Im}(\varphi_n^m)$, $\mathrm{Im}(\theta_n^m)$, a direct solution of the Pontryagin equations to obtain the optimal protocol is difficult. However, once we have a protocol from Monte Carlo simulations, consistency with the Pontryagin equations provides a valuable check. The equations of motion given in the main text for the dynamical variables can be derived from the Schrödinger equation $-i\partial_t \psi^m(x,t) = \mathcal{H}\psi^m(x,t)$ [see Eq. (2) of the main text], which leads to

$$\sum_{n=0}^{\infty} \begin{pmatrix} \dot{\varphi}_n \\ \dot{\theta}_n \end{pmatrix} g_n(\tilde{x}) = \sum_{n=0}^{\infty} \Big[\begin{pmatrix} \varphi_n \\ \theta_n \end{pmatrix} \dot{y}(t) g_n'(\tilde{x}) - u \begin{pmatrix} \varphi_n \\ -\theta_n \end{pmatrix} g_n'(\tilde{x}) + ib\tilde{x} \begin{pmatrix} \theta_n \\ \varphi_n \end{pmatrix} g_n(\tilde{x}) \Big], \tag{S8}$$

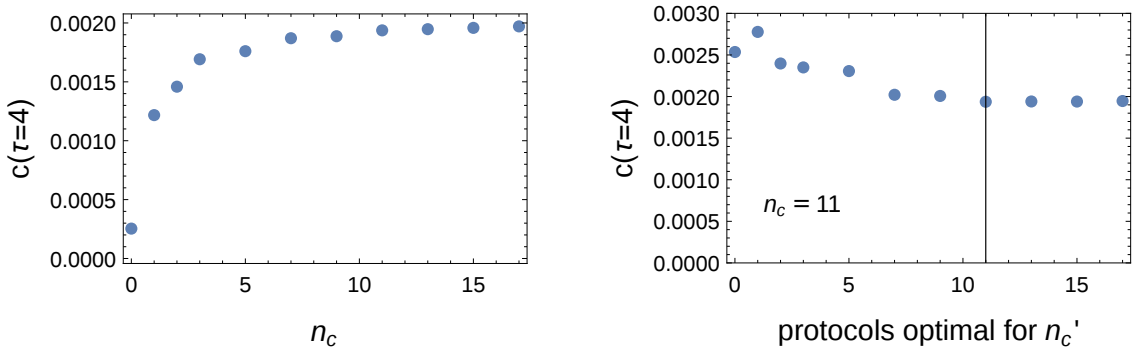

FIG. S2. Dependence of protocol performance on n_c for the example $\tau = 4/\omega$. Left panel: Change of the cost function with the included number of bound states n_c. Including more states increases the cost function, nevertheless, $c(\tau)$ seems to converge for large n_c. Right panel: Applying the cost function with $n_c = 11$ to protocols optimized for n_c'. Although the protocol optimized for $n_c' = n_c$ performs best, the differences to other protocols (showing different p) becomes minuscule in the regime of large n_c, n_c'.

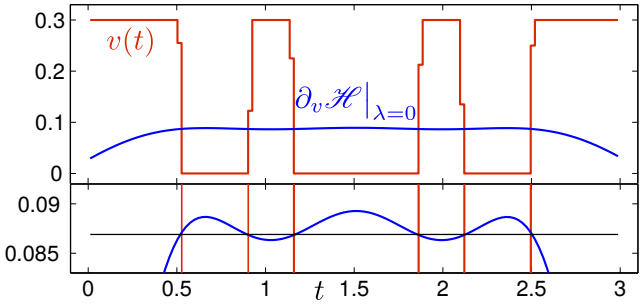

FIG. S3. Upper panel: An optimal protocol $v(t)$ for $\tau = 3$, $v_{\max} = 0.3$, $v_{\text{ave}} = 0.15$, $n_c = 7$ (red line). The coefficient of v in the optimal-control Hamiltonian $\mathscr{H}$ with the unknown Lagrange multiplier λ set to zero (blue curve). Lower panel: A zoom-in of the same plot. With a shift corresponding to λ the protocol can be determined by $\text{sgn}(\partial_v \mathscr{H})$.

where we have suppressed the superscript m for the dynamical variables and $\tilde{x} \equiv x - y(t)$. We now use the following properties of the Hermite polynomials $H_n'(z) = 2nH_{n-1}(z)$ and $zH_n(z) = nH_{n-1}(z) + \frac{1}{2}H_{n+1}(z)$ to write

$$g_n'(z) = \frac{1}{\xi}\left[\sqrt{\frac{n}{2}}g_{n-1}(z) - \sqrt{\frac{n+1}{2}}g_{n+1}(z)\right], \qquad zg_n(z) = \xi\left[\sqrt{\frac{n}{2}}g_{n-1}(z) + \sqrt{\frac{n+1}{2}}g_{n+1}(z)\right], \tag{S9}$$

which upon insertion into Eq. (S8), and using $\int_{-\infty}^{+\infty} g_n(x)g_m(x)dx = \delta_{nm}$, leads to the equations of motion in Eq. (7) of the main text. To evaluate the cost function at the end of the time evolution we expand the single-particle wave function $\psi^m(x,\tau)$ in terms of the domain-wall bound-state wave functions at position B as $\psi^m(x,\tau) = \sum_n \alpha_{m,n}^* \phi_n(x-\ell)$, where

$$\alpha_{m,n}^* = (\varphi_n^m - i\theta_n^m - i\varphi_{n-1}^m + \theta_{n-1}^m)/2, \qquad \alpha_{m,-n}^* = (\varphi_n^m - i\theta_n^m + i\varphi_{n-1}^m - \theta_{n-1}^m)/2, \qquad n > 0. \tag{S10}$$

With the knowledge of $\alpha_{m,n}$ the cost function can then be evaluated using Eqs. (S6) and (S7).

To verify the Pontryagin equations, we introduce conjugate momenta $\Pi_{\text{Re}(\varphi_n^m)}$, $\Pi_{\text{Re}(\theta_n^m)}$, $\Pi_{\text{Im}(\varphi_n^m)}$, $\Pi_{\text{Im}(\theta_n^m)}$ for each of the dynamical variables, write the optimal control Hamiltonian, and derive the equations of motion for the conjugate momenta (which turn out to be very similar to the equations of motions for the dynamical variables). Given the protocol, we find the dynamical variables as a functions of time. From the derivative of the cost function with respect to the dynamical variables, we obtain the final values of the conjugate momenta and evaluate them for all times by solving their equations of motion backward in time. We can then calculate $\partial_v \mathscr{H}$ up to the unknown Lagrange multiplier λ, which simply shifts this quantity. The consistency of our numerical protocols with Pontryagin's equations requires $\partial_v \mathscr{H} = 0$ at the jumps in the protocol (because this allows values of $v(t)$ different from 0 or $v_{\max}$). Without the knowledge of the shift by λ, this simply implies that $\partial_v \mathscr{H}$ must take the same values for *all* times that coincide with the jumps in the protocol, which is precisely what we obtain as shown in Fig. S3.